Texas Water Development Board

Report September 2011

UTBEST3D Hydrodynamic Model
Verification of Corpus Christi Bay

PI: Clint Dawson (The University of Texas at Austin)
E-mail: clint@ices.utexas.edu
Voice: (512) 475-8625

Team Members:

Clint Dawson, Professor

Jennifer Proft, Research Scientist

Vadym Aizinger, Visiting Research Scientist

Contents

List of Figures

1 Executive Summary

The University of Texas Bay and Estuary 3D (UTBEST3D) simulator solves the shallow water equations using a discontinuous Galerkin (DG) finite element method defined on unstructured prismatic meshes. The method is based on the use of discontinuous, piecewise polynomial approximating functions for each primary variable, defined over each element. The potential advantages of the DG method over more standard approaches include the ability to model flows at multiple scales, including resolution of long wave and advection-dominated flows, local (elementwise) mass conservation, and the ability to easily adapt the mesh and polynomial order locally. The flexibility of the code allows for both lower order and/or higher order polynomials to be used to approximate the solutions, by simply setting a parameter in the input file. The method is also scalable on parallel machines.

The overall objective of the project is to produce a calibrated model of Corpus Christi Bay and surrounding regions, by comparing simulated model results to real world recorded data provided by the TWDB. This comparison data includes elevation, salinity and velocity recordings at geographically specified locations for the year 2000. Additionally, a vertical convergence test to determine "the appropriate number of vertical layers for the run considering both convergence and runtime" is requested. Upon verification of the model in comparison to these specified datasets, a simulation of the year 2001 is to be conducted using a hotstart file from the previous year and an initial condition salinity file provided by the TWDB. Finally, the output data is to be provided to personnel in an agreed upon format to enable intermodel comparisons.

The TWDB provided boundary conditions (elevation forcing, river inflows, and specified salinity), finite element grid, initial salinity, baywide wind, precipitation, and evaporation data files which are used in these studies. Supporting scripts and additional features in the code are incorpoated to read and process the data files. Verification tests are performed using higher order approximations in space and baroclinic assumptions.

These tests reveal that the UTBEST3D code produces accurate water elevation and velocity results at specified recording stations when compared to real world data. Salinity comparisons yield doubts in the veracity of the comparison data and raise additional questions. Verification of the model is deemed successful for the year 2000, and year 2001 results are complete.

2 Model Description

2.1 Introduction

In this report, we discuss a recent application of the UTBEST3D (University of Texas Bay and Estuary 3D) simulator, which has been developed at UT Austin by the investigators. The UTBEST3D model development was motivated by the fact that, despite many recent advances in the development of simulators for modeling circulation in oceanic to continental shelf, coastal and estuarine environments, the search is still on for methods which are locally mass conservative, can handle very general types of elements, and are stable and higher-order accurate under highly varying flow regimes. Algorithms such as the discontinuous Galerkin method (DG) are of great interest within the ocean and coastal modeling communities; at a recent unstructured grid ocean modeling workshop, held in Halifax, Nova Scotia, many of the talks focused on applications of the DG method to three-dimensional ocean models. DG methods are promising because of their flexibility with regard to geometrically complex elements, use of shock-capturing numerical fluxes, adaptivity in polynomial order, ability to handle nonconforming grids, and local conservation properties; see [5] for a historical overview of DG methods.

In [1, 4], we investigated DG and related finite volume methods for the solution of the two-dimensional shallow water equations. Viscosity (second-order derivative) terms are handled in this method through the so-called local discontinuous Galerkin (LDG) framework [6], which employs a mixed formulation. Application of the methodology to three-dimensional shallow water models was described in [8, 2] and in a series of TWDB annual reports dating back to 2005. The 3D formulation is not a straightforward extension of the two-dimensional algorithm. In particular, it uses a special form of the continuity equation for the free surface elevation and requires postprocessing the elevation solution to smooth the computational domain.

The code was originally developed as a serial code. In a previous project, the code was parallelized for distributed memory clusters. The parallelization of the code is based on domain decomposition, whereby the global three-dimensional domain is split into subdomains. Each processor then computes the solution on its assigned subdomain, and shares information with neighboring subdomains using MPI (message passing interface). Because of the local nature of the DG scheme, and the use of explicit time-stepping, the code scales well in parallel. Tests for efficiency and accuracy were previously conducted for similar but simplified test cases.

Application to the simulation of tide-driven flows in Corpus Christi Bay was conducted, based on input data supplied by the TWDB. Additional supporting scripts and features have been incorporated into the code, including time-varying open sea boundary data, wind, salinity, evaporation and precipitation data for a baroclinic model, some of which are presented in a previous report.

The rest of this report is organized as follows. In the next section, we briefly review the modeling assumptions used in the code, describe the flow equations, boundary conditions, and turbulence closure models. We then give an overview of the code itself, including a description of the necessary UTBEST3D input files. Finally, verification studies of the calibrated model for Corpus Christi Bay and surrounding regions are presented and conclusions discussed.

2.2 Model and assumptions

For $\mathbf{a}, \mathbf{b} \in \mathbb{R}^d, \mathbf{c} \in \mathbb{R}^e$, we denote by $\mathbf{ac}$ the tensor-product of $\mathbf{a}$ and $\mathbf{c}$ and by $\mathbf{a} \cdot \mathbf{b}$ the dot-product of $\mathbf{a}$ and $\mathbf{b}$.

Let $\Omega(t) \subset \mathbb{R}^3$ be the time-dependent domain. We assume the top boundary of the domain $\partial\Omega_{top}(t)$ is the only moving boundary. The bottom $\partial\Omega_{bot}$ and lateral $\partial\Omega_D(t)$ boundaries are assumed to be fixed (though the height of the lateral boundaries can vary with time according to the

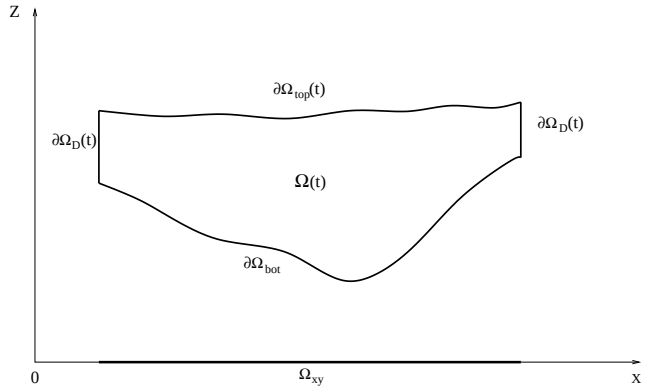

Figure 1: Vertical cross-section of the computational domain $\Omega(t)$.

movements of the free surface). We also require the lateral boundaries to be strictly vertical (see Figure 1). The last requirement is only needed to assure that the horizontal cross-section of the domain $\Omega(t)$ (denoted by Ω_{xy}) doesn't change with time.

Keeping in line with the specific anisotropy of $\Omega(t)$ we construct a 3D finite element mesh by extending a 2D triangular mesh of Ω_{xy} in the vertical direction, thus producing a 3D mesh of $\Omega(t)$ that consists of one or more layers of prismatic elements. In order to better reproduce the bathymetry and the free surface elevation of the computational domain we do not require top and bottom faces of prisms to be parallel to the xy-plane, although the lateral faces are required to be strictly vertical.

For a point $(x, y) \in \Omega_{xy}$ we denote by $z_b(x, y)$ the value of the z-coordinate at the bottom of the domain and by $\xi_s(t, x, y)$ at the top. A key feature of the 3D LDG model is the fact that all primary variables, including the free surface elevation, are discretized using discontinuous polynomial spaces. As a result, computed values of the free surface elevation may have jumps across inter-element boundaries. If the finite element grids were to follow exactly the computed free surface elevation field this would cause the elements in the surface layer to have mismatching lateral faces (staircase boundary). We avoid this difficulty by employing a globally continuous free surface approximation that is obtained from the computed values of the free surface elevation ξ with the help of a smoothing algorithm (see Figure 2). Thus H is the computed height of the water column, and H_s is the postprocessed height.

It must be noted here that solely the computational mesh is modified by the smoothing algorithm whereas the computed (discontinuous) approximations to all unknowns, including the free surface elevation, are left unchanged. This approach preserves the local conservation property of the LDG method and is essential for our algorithm's stability.

2.3 3D baroclinic shallow water equations

The momentum equations in conservative form are given by [14]

$$\partial_t \mathbf{u}_{xy} + \nabla\cdot(\mathbf{u}_{xy}\mathbf{u} - \mathcal{D}\nabla\mathbf{u}_{xy}) + g\nabla_{xy}\xi + \frac{g}{\rho_0}\nabla_{xy}\int_z^{\xi}(\rho(T,S,\xi-\tilde{z})-\rho_0)d\tilde{z} - f_c\mathbf{k}\times\mathbf{u}_{xy} = \mathbf{F}, \quad (1)$$

where ρ_0 is the reference density and $\rho(T, S, p)$ is the density computed from the equation of state. The wind stress, atmospheric pressure gradient, and tidal potential are combined into a body force term $\mathbf{F}$, $\nabla_{xy} = (\partial_x, \partial_y)$, ξ is the value of the z coordinate at the free surface, $\mathbf{u} = (u, v, w)$ is the velocity vector, $\mathbf{u}_{xy} = (u, v)$ is the vector of horizontal velocity components, f_c is the Coriolis

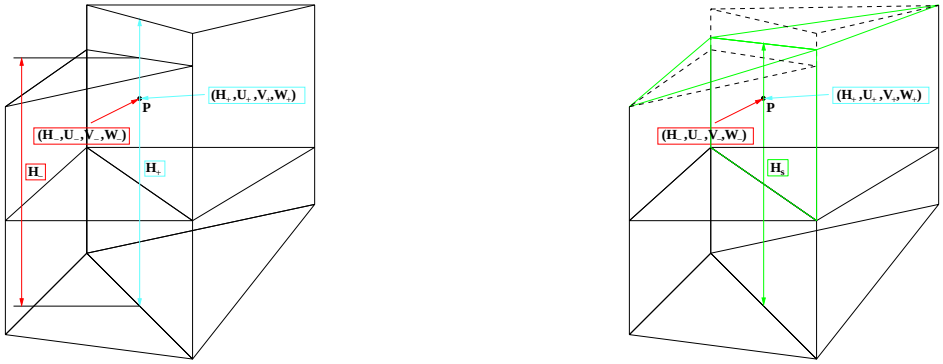

Figure 2: Free surface approximation before mesh smoothing (left) and after (right)

coefficient, $\mathbf{k} = (0, 0, 1)$ is a unit vertical vector, g is acceleration due to gravity, and $\mathcal{D}$ is the tensor of eddy viscosity coefficients defined as follows:

$$\mathcal{D} = \begin{pmatrix} D_u & 0 \\ 0 & D_v \end{pmatrix}, \tag{2}$$

with D_u, D_v 3×3 symmetric positive-definite matrices, and $\mathcal{D}\nabla \mathbf{u}_{xy} = \begin{pmatrix} D_u \nabla u \\ D_v \nabla v \end{pmatrix}$. In particular,

$$D_u \;=\; D_v \;=\; \begin{pmatrix} A_x & 0 & 0 \\ 0 & A_y & 0 \\ 0 & 0 & \nu_t \end{pmatrix},$$

where A_x, A_y are the horizontal and ν_t is the vertical eddy viscosity coefficient.

The equation of state used in UTBEST3D is due to Klinger [11] and is given by

$$\rho(T, S, p) \;=\; C(p) + \beta(p)S \;-\; \alpha(T, p)T \;-\; \gamma(T, p)(35 - S)T, \tag{3}$$

where

$$C \;=\; 999.83 \;+\; 5.053p \;-\; 0.048p^2, \tag{4}$$
$$\beta \;=\; 0.808 \;-\; 0.0085p, \tag{5}$$
$$\alpha \;=\; 0.0708(1 \;+\; 0.351p \;+\; 0.068(1 - 0.0683p)T), \tag{6}$$
$$\gamma \;=\; 0.003(1 \;-\; 0.059p \;-\; 0.012(1 - 0.064p)T). \tag{7}$$

p is the height of the water column above the point expressed in kilometers, T is the temperature in degrees Celsius, and S is the salinity in psu.

The continuity equation is

$$\nabla \cdot \mathbf{u} \;=\; 0. \tag{8}$$

2.4 Boundary conditions

The following boundary conditions are specified for the system:

- At the bottom boundary $\partial\Omega_{bot}$, we have no normal flow

$$\mathbf{u}(z_b) \cdot \mathbf{n} = 0 \tag{9}$$

and the quadratic slip condition for the horizontal velocity components

$$\nu_t \frac{\partial u}{\partial z}(z_b) = C_f \sqrt{u^2(z_b) + v^2(z_b)} u(z_b), \tag{10}$$

$$\nu_t \frac{\partial v}{\partial z}(z_b) = C_f \sqrt{u^2(z_b) + v^2(z_b)} v(z_b), \tag{11}$$

where $\mathbf{n} = (n_x, n_y, n_z)$ is an exterior unit normal to the boundary.

- The free surface boundary conditions with the rates of precipitation (q_p) and evaporation (q_p) specified in velocity units have the form

$$\partial_t \xi \ + \ u(\xi) \ \partial_x \xi \ + \ v(\xi) \ \partial_y \xi \ - \ w(\xi) \ = \ q_p \ - \ q_e, \tag{12}$$

and

$$\nabla u(\xi) \cdot \mathbf{n} \ = \ \nabla v(\xi) \cdot \mathbf{n} \ = \ 0 \tag{13}$$

in the case of no wind. In the presence of wind forcing however, the last equation is replaced by

$$\nu_t \frac{\partial \mathbf{u}}{\partial z}(\xi) = \tau_{\mathbf{s}}, \tag{14}$$

where $\tau_{\mathbf{s}}$ is the surface stress which can be specified directly or computed from the wind velocity at 10m above the water surface, $\mathbf{U}_{10}$, by

$$\tau_{\mathbf{s}} \ = \ \frac{\rho_a}{\rho_0} C_s |\mathbf{U}_{10}| \mathbf{U}_{10} \tag{15}$$

with $C_s = 10^{-3}(A_{W1} + A_{W2}|\mathbf{U}_{10}|)$ for $U_{low} \leq |\mathbf{U}_{10}| \leq U_{high}$ and C_s held constant at the extremal values outside of this interval. Similarly to [17] we set $A_{W1} = 0.1$, $A_{W2} = 0.063$, $U_{low} = 6\ m/s$, $U_{high} = 50\ m/s$.

On the lateral boundaries, we consider several common types of boundary conditions:

- Land boundary: No normal flow

$$u_{\mathbf{n}} = \mathbf{u} \cdot \mathbf{n} = 0, \tag{16}$$

and zero shear stress

$$\nabla u_{\boldsymbol{\tau}} \cdot \mathbf{n} \ = \ 0, \tag{17}$$

where $\boldsymbol{\tau}$ and $\mathbf{n}$ denote a unit tangential and a unit exterior normal vectors to the boundary, correspondingly.

- Open sea boundary: Zero normal derivative of the horizontal velocity components

$$\nabla u \cdot \mathbf{n} \ = \ \nabla v \cdot \mathbf{n} \ = \ 0, \tag{18}$$

and prescribed surface elevation $\xi_{os}(x, y, t)$

$$\xi = \xi_{os}(x, y, t). \tag{19}$$

- River boundary: Prescribed velocities

$$\mathbf{u} = \mathbf{u}_r, \tag{20}$$

and prescribed surface elevation

$$\xi = \xi_r. \tag{21}$$

- Radiation boundary: Zero normal derivative of the horizontal velocity components

$$\nabla u \cdot \mathbf{n} \;=\; \nabla v \cdot \mathbf{n} \;=\; 0. \tag{22}$$

Analytically, the free surface elevation can be computed from (12). However, a computationally more robust method [14] is obtained by integrating continuity equation (8) over the total height of the water column. Taking into account boundary conditions (9) – (12) at the bottom and top boundaries we arrive at a 2D equation for the free surface elevation commonly called the primitive continuity equation (PCE),

$$\partial_t \xi \;+\; \partial_x \int_{z_b}^{\xi} u dz \;+\; \partial_y \int_{z_b}^{\xi} v dz \;=\; q_p \;-\; q_e. \tag{23}$$

2.5 Species transport

Species transport equations for salinity, temperature and turbulence quantities are included in the model. Transport is described by advection-diffusion equations of the form

$$r_t + \nabla \cdot (\mathbf{u} r) - \nabla \cdot (K_r \nabla r) = f, \quad \Omega(t) \times (0, T), \tag{24}$$

where $r = S$ for salinity or $r = T$ for temperature, and $K_r = \begin{pmatrix} \tilde{A}_x & 0 & 0 \\ 0 & \tilde{A}_y & 0 \\ 0 & 0 & \nu_r \end{pmatrix}$ is a specified diffusion tensor. These equations must be supplemented with initial and boundary conditions. The DG method is also applied to the solution of these equations. Precipitations/evaporation effects on salt balance are incorporated with the help of the virtual salinity flux boundary condition at the free surface. This approach is based on replacing fluxes of fresh water due to precipitation and evaporation by equivalent fluxes of salt:

$$S(\xi) w(\xi) = \; -(q_p \;-\; q_e) S(\xi) \tag{25}$$

or equivalently

$$S(\xi) \mathbf{u}(\xi) \cdot \mathbf{n} = \; -(q_p \;-\; q_e) n_z S(\xi) \tag{26}$$

This boundary condition is applied to the transport equation for salt concentration and does not affect any other parts of code as opposed to the 'direct' incorporation of the fresh water flux that would require a computationally expensive inforcement of salt balance. However, the virtual salinity flux method does not guarantee the exact conservation of salt and therefore may cause some problems in long term simulations.

2.6 Turbulence

UTBEST3D provides vertical eddy viscosity models of various levels of computational and conceptual complexity. In order of increasing complexity those include a constant eddy viscosity coefficient, an algebraic (zeroth order) model, as well as one and two equation models.

- The simplest model amounts to explicitly specifying diagonal entries to the tensors of eddy viscosity/diffusivity coefficients for all variables in (1) and (24).

- Two algebraic models implemented in UTBEST3D are due to Davies [7] and give good results at a reasonable computational cost in cases where accurate vertical resolution of flow is not important.

  In the first algebraic model the eddy viscosity and diffusivity coefficients are set equal to $C_t \frac{(\bar{u}^2+\bar{v}^2)}{\omega_a}$, where $\bar{u}$ and $\bar{v}$ are depth averaged horizontal velocity components, $C_t = 2 \times 10^{-5}$ is a dimensionless coefficient, and ω_a a typical long wave frequency set to $10^{-4} s^{-1}$.

  Model two is very similar to model one, except that the eddy viscosity is assumed to be proportional to $H\sqrt{\bar{u}^2 + \bar{v}^2}$.

- The first order vertical eddy viscosity closure model solves a transport equation for the turbulent kinetic energy in addition to the mass, momentum, and species transport equations.

$$k_t + \nabla \cdot (\mathbf{u}k) - \frac{\partial}{\partial z}(\nu_k \frac{\partial}{\partial z} k) = \nu_t \left(\left(\frac{\partial u}{\partial z} \right)^2 + \left(\frac{\partial v}{\partial x} \right)^2 \right) + \nu_r \frac{g}{\rho_0} \frac{\partial \rho}{\partial z} - \epsilon, \tag{27}$$

  where ν_k is the vertical diffusivity coefficient for k and $\epsilon = (C_\mu^0)^3 k^{\frac{3}{2}} l^{-1}$ is the dissipation rate of the turbulent kinetic energy. The turbulent mixing length l is computed algebraically in this model and is set equal to $l(z) = \kappa\,(z - z_b)\,\sqrt{\xi - z}\,F_l(Ri)$ (see Delft3D-Flow manual [9]). $C_\mu^0 = \sqrt{0.3}$ is a calibration constant, $\kappa = 0.4$ is the von Karman constant, and $F_l(Ri)$ is the damping function accounting for stratification effects. F_l depends on the gradient Richardson number

$$Ri = \frac{-\frac{g}{\rho_0}\frac{\partial \rho}{\partial z}}{\left(\frac{\partial u}{\partial z}\right)^2 + \left(\frac{\partial v}{\partial x}\right)^2} \tag{28}$$

  and is of the form:

$$F_l(Ri) = \begin{cases} e^{-2.3Ri}, & Ri \geq 0, \\ (1 - 14Ri)^{0.25}, & Ri < 0. \end{cases} \tag{29}$$

  Once k is computed one can obtain the vertical eddy viscosity and diffusivity coefficients by taking $\nu_t = C_\mu^0 k^{\frac{1}{2}} l$ and $\nu_r = \nu_k = \frac{\nu_t}{0.7}$ correspondingly. Neumann type boundary conditions for k are used at the free surface and the sea bed $\nu_k \frac{\partial k}{\partial n} = 0$.

- The second order closure model implemented in UTBEST3D is based on the generic turbulence length scale model proposed by Warner et al [15]. The main advantage of this formulation is the ability to switch between several two equation models, including $k - \epsilon$ and Mellor-Yamada, by changing a few constant parameters. In addition to the transport equation for k, this model includes a second transport equation for derived quantity ψ

$$\psi_t + \nabla \cdot (\mathbf{u}\psi) - \frac{\partial}{\partial z}(\nu_\psi \frac{\partial}{\partial z}\psi) = \frac{\psi}{k} \left(C_1 \nu_t \left(\left(\frac{\partial u}{\partial z} \right)^2 + \left(\frac{\partial v}{\partial x} \right)^2 \right) + C_3 \nu_r \frac{g}{\rho_0} \frac{\partial \rho}{\partial z} - C_2 \epsilon F_{wall} \right), \tag{30}$$

  where $\psi = (C_\mu^0)^p k^m l^n$ and C_3 is equal to C_3^- for stably stratified flow and C_3^+ otherwise. Depending on the choice of p, m, and n we obtain different closure schemes. The turbulent mixing length is computed using k and ψ. The eddy viscosity and diffusivity coefficients are obtained from $\nu_t = \sqrt{2} S_m k^{\frac{1}{2}} l$ and $\nu_r = \sqrt{2} S_h k^{\frac{1}{2}} l$, where S_m and S_h are stability functions given by:

$$S_h = \frac{0.4939}{1 - 30.19 G_h}, \qquad S_m = \frac{0.392 + 17.07 S_h G_h}{1 - 6.127 G_h}, \tag{31}$$

where $G_h = G_{h_u} - \frac{(G_{h_u}-G_{h_c})^2}{G_{h_u}+G_{h0}-2G_{h_c}}$ and $G_{h_u} = \min(G_{h0}, \max(-0.28, \frac{g}{\rho_0}\frac{\partial \rho}{\partial z}\frac{l^2}{2k}))$ with $G_{h0} = 0.0233, G_{h_c} = 0.02$.

To improve stability properties of the two-equation model we employ Neumann boundary conditions for ψ at the free surface $\nu_\psi \frac{\partial \psi}{\partial z} = -n\nu_\psi (C_\mu^0)^p k^m \kappa l_s^{n-1}$ and at the sea bed $\nu_\psi \frac{\partial \psi}{\partial z} = n\nu_\psi (C_\mu^0)^p k^m \kappa l_b^{n-1}$, where the turbulent mixing length is derived from the law of the wall: $l_s = l_{|_{\xi_s}} = z_1 e^{\frac{\kappa |u|}{\tau_s}}$ and $l_b = l_{|_{z_b}} = z_0 \frac{\kappa}{\sqrt{Cf}}$ with C_f being as in (11) and z_1 the surface roughness coefficient.

Values of the parameters for four popular two equation models are shown in Table 1. Discretization of (30) is also done similarly to (24).

	Mellor-Yamada [12]	$k-\epsilon$ [3]	$k-\omega$ [16]	generic [13]
p	0	3	-1	2
m	1	1.5	0.5	2
n	1	-1	-1	2/3
ν_k	$\frac{\nu_t}{2.44}$	ν_t	$\frac{\nu_t}{2}$	$\frac{\nu_t}{0.8}$
ν_ψ	$\frac{\nu_t}{2.44}$	$\frac{\nu_t}{1.3}$	$\frac{\nu_t}{2}$	$\frac{\nu_t}{1.07}$
C_1	0.9	1.44	0.555	1
C_2	0.5	1.92	0.833	1.22
C_3^+	1	1	1	1
C_3^-	2.53	-0.52	-0.58	0.1
k_{min}	7.6e-6	7.6e-6	7.6e-6	7.6e-6
ψ_{min}	1e-8	1e-8	1e-8	1e-8
F_{wall}	$1 + 1.33\left(\frac{l}{z-z_b}\right)^2 + 0.25\left(\frac{l}{\xi_s - z}\right)^2$	1	1	1

Table 1: Generic turbulence closure model parameters.

3 Description of the UTBEST3D code

Descriptions of the model have been described in previous TWDB reports. Nonetheless, we include some details herein for the purpose of completeness. The UTBEST3D code is based on a discontinuous Galerkin discretizaton; that is, each unknown variable is approximated as a discontinuous, piecewise polynomial, the degree of which is chosen by the user. At each time step, the solution is advanced in time using explicit Runge-Kutta methods. For piecewise constant spatial approximations, a forward Euler method is used for temporal integration; for piecewise linear approximations, a second order Runge-Kutta method is used, etc.

Input to the code consists of four files, which are named fort.14, fort.15, fort.17 and utbest_config.inp. The fort.14 and fort.15 files are modeled after input files used for ADCIRC, ELCIRC and SELFE. The full description of these files is given in the user's manual, but briefly:

- fort.14–contains finite element mesh (nodes and elements) information for the 2D grid, node numbers and coordinates, element-to-node connectivity
- fort.15–contains 2D run parameters, time step information, output specifications
- fort.17–contains finite element edge information needed for the DG method; edge numbering, nodes connected to an edge, elements on each side of the edge, types of boundary conditions specified on the boundary edges

- utbest_config.inp–contains additional run parameters needed for the 3D code, locations of input/output files, turbulence options, number of vertical layers, and order of approximation used in the DG method.

The model has been parallelized using domain decomposition and MPI. The 2D projection Ω_{xy} of the 3D domain Ω is partitioned into overlapping subdomains using the METIS library [10]. Each subdomain has a one-to-one correspondence with a compute processor. A partitioning code was written which reads in the two-dimensional mesh information contained in fort.14 and fort.17 and passes this information to METIS, which uses an algorithm to divide the global grid into local grids for each subdomain. The partitioning code creates new input files fort_np*xxx*.14 and fort_np*xxx*.17, where *xxx* is the total number of subdomains. The local grid information for each processor is contained in these files. On each subdomain, the elements/nodes are renumbered from one to the number of elements/nodes contained in the subdomain. The preprocessor creates additional files fort_np*xxx*.18 and fort_np*xxx*.offset. The first file contains information about the local-to-global element numbering and the message passing information from one subdomain to its neighbors, while the second file is a binary file used in MPI–I/O routines in UTBEST3D. When running in parallel, each processor reads its grid information from fort_npxxx.14 and fort_npxxx.17 and its message passing information from fort_npxxx.18. The information contained in fort.15 is global information which is common to each processor. At each stage in the Runge-Kutta scheme, MPI is used to pass element solution information among the subdomains. Since the code is fully explicit, no global systems of equations must be solved and no global information must be broadcast to all of the processors; furthermore, the DG scheme is very local and only requires nearest neighbor communications. Therefore, the parallel speed-up of the code is quite good.

4 Verification Studies

The overall objective of the project is to produce a calibrated model of Corpus Christi Bay and surrounding regions, by comparing simulated model results to real world recorded data provided by the TWDB. This comparison data includes elevation, salinity and velocity results at specified locations. A "vertical convergence test to determine the appropriate number of vertical layers for the run considering both convergence and runtime" is requested. Upon verification of the model in comparison to these year 2000 specified datasets, a simulation of the year 2001 is requested using a hotstart file from the previous year and a spatially defined initial salinity file provided by TWDB. Finally, the output data is to be provided to the TWDB in an agreed upon format to enable comparisons with other shallow water models. In order for TWDB personnel to conduct these comparisons, pertinant input information to run the UTBEST3D code is necessary to define.

We performed our simulations on the region shown in Figure 3. Both model input files, such as the finite element mesh, as well as output comparison data files are provided by TWDB. The input data included inflow velocities at 11 specific riverine and powerplant locations in and around Corpus Chrisi Bay, and elevation and salinity data boundary conditions at Bob Hall Pier. Baywide-defined meteorological data included wind data from the NOAA Ingleside station, precipitation measured at the Naval Air Station, and salinity initial conditions based on a TXBLEND model run. Alternatively, comparison to real-world data included water level elevation at 12 points and salinity data at 10 points definted in Table 3. Herein we present and research the validity of our model results to this comparison data.

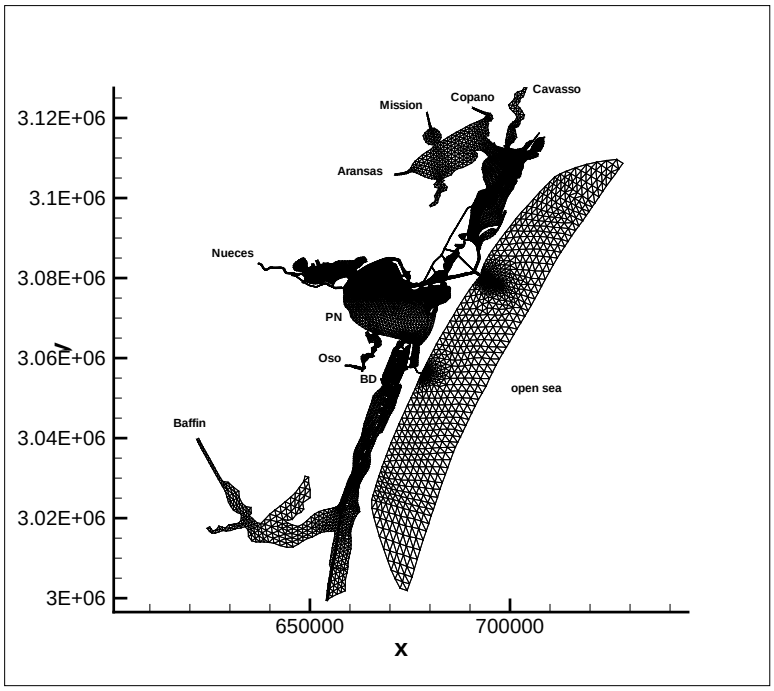

Figure 3: Aerial view of the domain showing the open sea boundary and locations of the various rivers and power plants

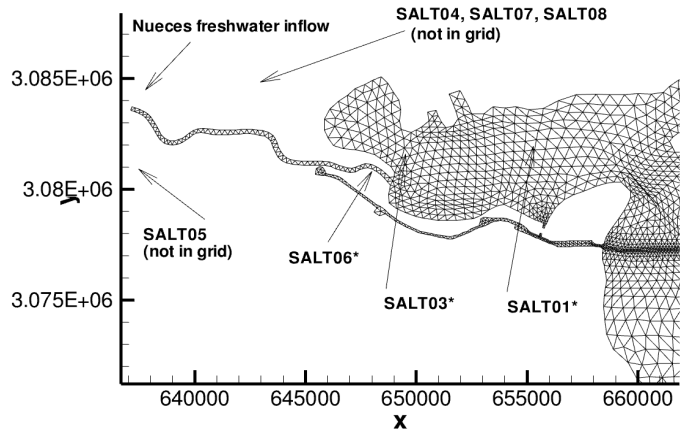

Figure 4: Finite element mesh around Nueces Bay showing the locations of tcSALT* stations

4.1 Model Data Input and Parameters

Files provided by TWDB are generated from various internal and external data sources and contain data for at least the years 2000 and 2001. In some cases, the files contain data from earlier and

later years as well.

Ocean tidal water elevation boundary conditions (tc014bobhall.wlevel.txt) are taken directly from recordings maintained by the National Oceanic and Atmospheric Administration located at Bob Hall Pier, 27° 34' 51" N, 97° 12' 59" W. Although the data is provided in MSL datum, it is converted to NAVD88 which is only 0.017m above MSL.

Wind data (tc006ingle.wind.txt) was recorded at the Ingleside station near the northeast portion of Corpus Christi Bay, 27° 49' 18" N, 97° 12' 11" W. This data was assumed to be baywide, hence defined as a spatially constant but temporally varying quantity. Precipitation and evaporation rates (precipcorpus.txt, evapcorpus.txt) are measured at the Naval Air Station near 27° 47' N, 97° 31' W and are also defined baywide. Note that each of these datasets are defined as an average value for a very large area and therefore may have inherent errors in them.

Initial conditions for salinity (2000_InitialSalinity.txt, 2001_InitialSalinity_FromTXBLEND.txt) are generated from a TWDB internal TXBLEND model run. Though potentially highly accurate, the data has not yet been verified using field data. Data for 11 river inflow locations and two power plant discharge/intake locations (location_inflow.txt) are included in the model. The rivers and powerplants, initial temperature and (estimated) initial salinity data are given in Table 2, the approximate locations of which are labeled in Figure 3. Salinity boundary conditions are defined on the open ocean (gnsaloffptarn.txt).

River/power plant	Temperature (c)	Initial salinity (ppt)
Cavasso	20	0
Copano	20	0
Mission	20	0
Aransas	20	0
Nueces	20	0
PwrNue discharge	20	19
PwrNue intake	20	19
Oso	20	0
BD discharge	20	31.9
BD intake	20	31.9
Baffin	20	0

Table 2: Inflow/outflow locations, temperature and initial salinity for Corpus Christi Bay

All given input data from TWDB was converted to appropriate units and formats for use in the UTBEST3D code. The converted evaporation, precipitation, wind and salinity boundary condition are displayed in Figure 5. We note that the elevation data is converted to NAVD88, as well as the comparison data for "tc" water elevation locations. The values of the initial salinity specifically at the powerplant discharge and intake points are estimated from the baywide initial salinity file provided by TWDB. Furthermore, a time dependent salinity flux at these locations is input to the model, based on a previous run for the year 2000 using piecewise constant basis functions.

As outlined in section "Description of the UTBEST3D code", input data to the model also includes finite element grid file fort.14, 2D run parameter file fort.15, finite element edge file fort.17 and additional 3D run parameters in utbest_config.inp. For this baroclinic flow scenario, a $k-\epsilon$ turbulence closure model is used to compute the vertial eddy viscosity. Thus, we are solving for variables u, v, w, ξ, S, T, k and ϵ. Piecewise linear approximations are constructed for all variables. Note that salinity is tempered with a slope limiter. Based on previous simulations, a stable time

step of 0.5 seconds is utilized. The solution is advanced in time and space using an explicit second order Runge-Kutta method. The majority of physical parameters are chosen on the basis of previous calibration runs, such as the bottom friction (0.05) and bottom roughness (0.01) parameters. The specified tidal forcing that is imposed at the open sea is ramped up over a 2 day period.

The finite element model is defined on a three dimensional mesh through the implementation of layers in the bathymetry. Layers are defined to be equidistant, and therefore the local number of layers depends on the local bathymetry. Mesh grading parameters specified in the file utbest_control.inp control the minimum height of the bottom most element, which are often much smaller than elements in complete layers, as a fraction of the full layer height. If the the height of the bottommost element is smaller than a given value, it is merged with the element immediately above. For a one layer simulation, the 3D mesh contains a total of 35324 prismatic elements.

We added features to UTBEST3D to read and process the given data files for use in the code, such as a linear interpolation between specified data points in time. Additionally, we wrote supporting scripts to convert the recorded data into an input format for UTBEST3D and an output format requested by TWDB personnel.

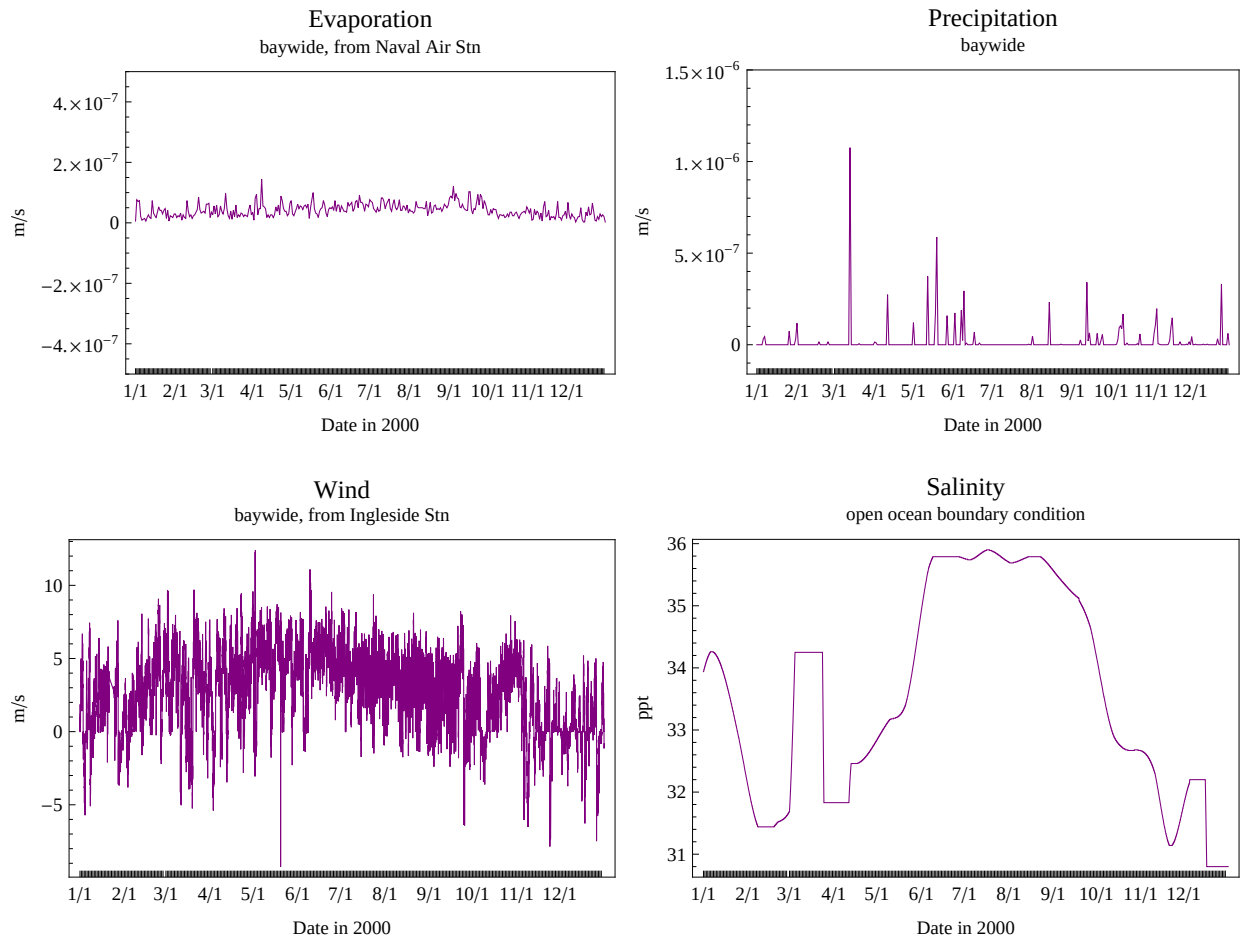

Figure 5: Input data (converted to UTBEST3D units)

4.2 Numerical Results

Elevation, salinity and temperature are measured at various locations defined in Table 4 and compared to recorded data. A figure of pertinent locations is displayed in Figure 6. As stated by TWDB personnel, comparison data for locations marked "tc" are considered highly accurate and datum corrected. This is not the case for locations marked "twdb" which contain outliers and occasional extended periods of missing data which have not yet been verified and quality controlled. Consequently we are not confident in the comparison data at those locations and simply present the results without detailed interpretation. As the UTBEST3D model is run with a datum of NAVD88, the water elevation comparison data recorded in MSL is therefore converted to NAVD88, a difference of only 0.017m.

We note that points 13 and 17 are ignored in our numerical results since they do not fall within the model domain. Figure 3 displays an aerial view of the domain showing the recording locations. In generating the figures below, we printed UTBEST3D solutions at intervals of 28800 time steps (four hours). Comparison data is provided at different intervals depending on the quantity measured. The plotting package generating the figures (Mathematica) linearly interpolates between points.

	File	Location	Recorded quantity
1	tc001ccnas	CC Naval Air Stn	Water Level
2	tc005packchan	Packery Channel	Water Level
3	tc006ingle	Ingleside	Water Level
4	tc008txaqu	Texas Aquarium	Water Level
5	tc009ptaran	Port Aransas	Water Level
6	tc011whitept	White Point	Water Level
7	tc014bobhall	Bobhall Pier	Water Level
8	tc015rockpt	Rockport	Water Level
9	twdb-aransas	Aransas Bay	Water Level, Salinity
10	twdb-corpus	Corpus Christi Bay	Water Level, Salinity
11	twdb-lagunajfk	Laguna Madre	Water Level, Salinity
12	twdb-lagunaupbaff	Baffin Bay	Water Level, Salinity
13	twdb-lavaca	not in grid	Salinity
14	tcSALT01	Nueces Bay	Salinity
15	tcSALT03	Nueces Bay	Salinity
16	tcSALT04	not in grid	Salinity
17	tcSALT05	not in grid	Salinity
18	tcSALT08	not in grid	Salinity

Table 3: Files, locations, and quantities measured

Complementary to the figures contained herein, we constructed a GoogleMaps API to display the results geographically on a map of features and locations. This technology can be made available via a webpage.

In each of the following figures, recorded data is displayed in black, and UTBEST3D numerical results are blue for water elevation, green for salinity, and orange for velocity. Note that the vertical scale varies in each plot, depending on the magnitude of the solution in each location. Unless otherwise indicated, the remaining figures presented in this report pertain to the one-layer run.

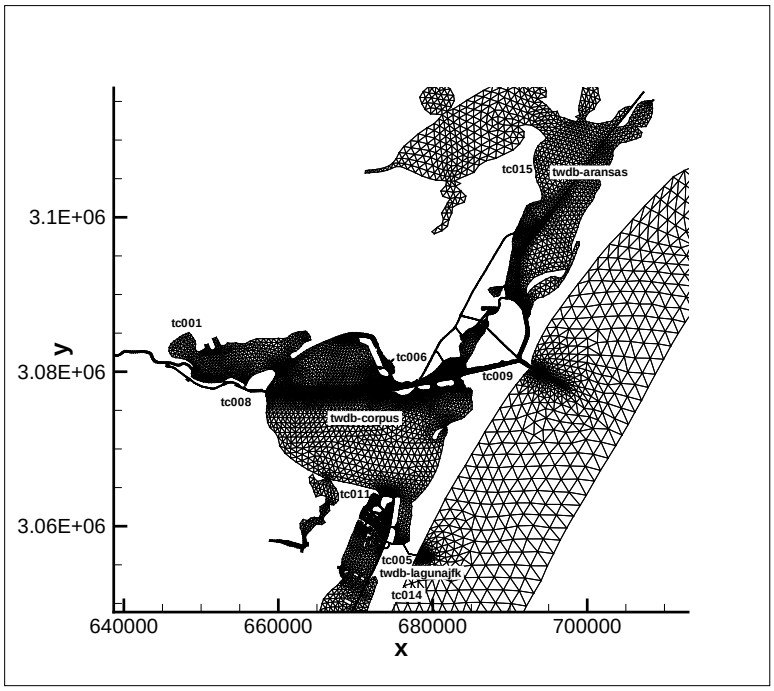

Figure 6: Aerial view of the domain showing the recording locations

4.2.1 Water elevation

For locations marked by "tc", Figures 7-8 indicate that the model results match well with the recorded data. The phasing is virtually identical, and we capture the water level adjustments very well. Note that the height above datum (NAVD88) is in meters. In general, we tend to underpredict the tidal level itself, a characteristic that is increasingly evident as the solution propogates deeper into the channel. The source of this dampening needs further investigation.

However, a comparison of results at locations marked "twdb" are unreliable, as expected. There appear to be some datum issues associated with the recorded data, and the recording device clearly fails at certain times. In an effort to partially address these datum issues, we consider shifting the model output and plotting against the recorded data. To do so, we calculated the average value of the output over the period of time for each twdb station, compared this to the average value of the recorded data over the entire year time period (neglecting visually obvious outliers) and shifted the graph by the difference. For example, the station "twdb-aransas" has a model output average value of -0.052019 over the simulation period, as can been seen by the solid blue line in Figure 9; the average value calculated over the year 2000 for the recorded data is 2.31427. By shifting the graph of the UTBEST output by the difference between these amounts, we see an interesting trend. The comparisons are somewhat similar up to February of 2000, when the recording device seems to have failed. The recorded data is again retrieved in early March, albeit with a shifted datum, yielding a more accurate phasing and water level during this timeframe. The graphs of similarly shifted comparisons at other "twdb" locations are in Figure 10, where we have attempted to neglect obvious outliers in the calculation of the average value.

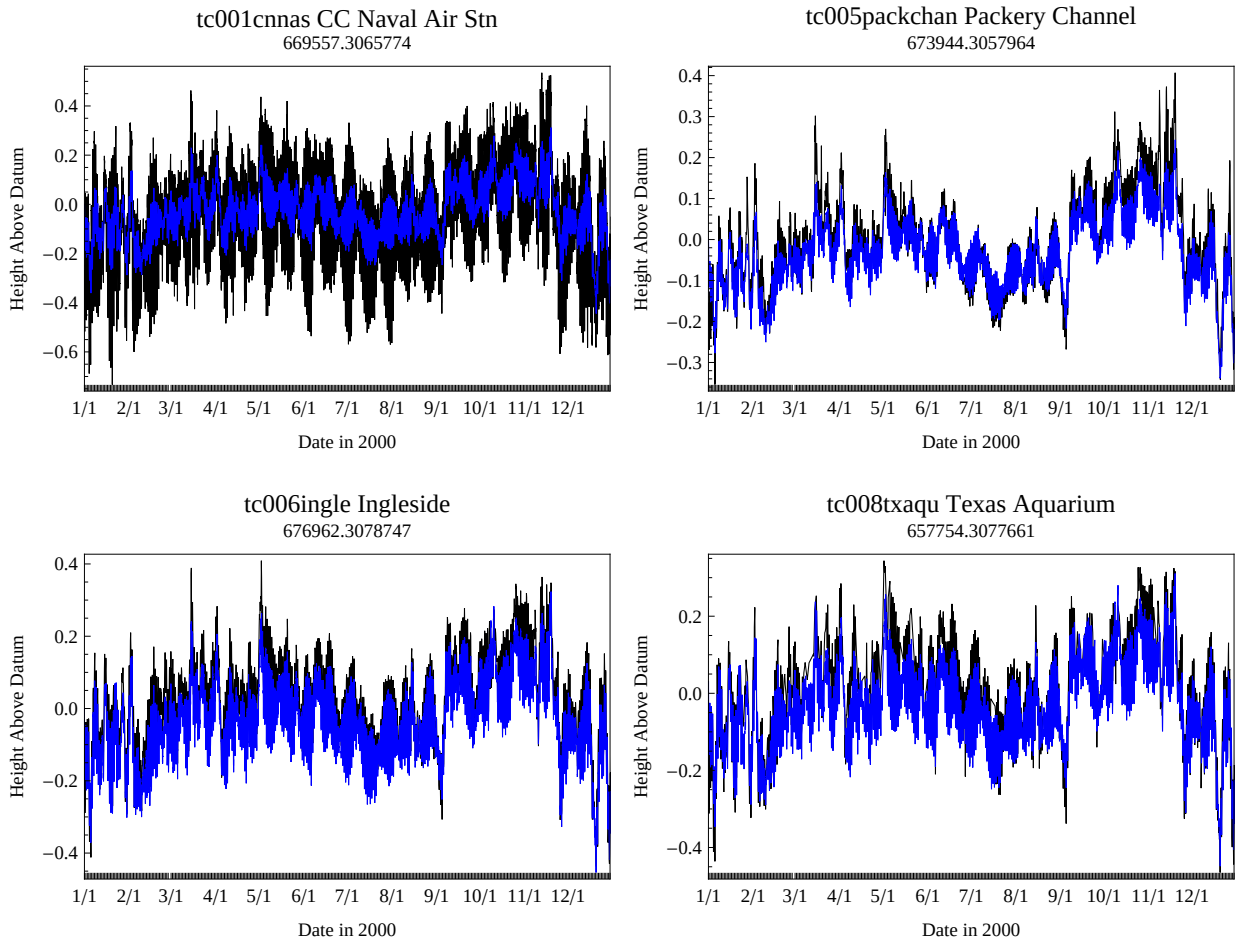

Figure 7: Water elevation comparisons at "tc" locations

4.2.2 Salinity

The UTBEST model is baroclinic with the ability to incorporate salinity data. Initial conditions for salinity at start times January 1, 2000 and 2001 are each generated from an internal TXBLEND model run. The specified inflow values are freshwater (zero salinity) at all riverine locations. To specify the salinity value at powerplant discharge locations, we initially run a piecewise constant solution simulation and record the salinity value as an input for the final piecewise linear run.

Salinity values are requested by TWDB at locations listed in Table 3. We note, however, that twdb-lavaca, tcSALT04, tcSALT05, and tcSALT08 are not within the defined finite element grid. Therefore the salinity values at these locations cannot be accurately provided. Our results are presented in Figures 11-12.

Though potentially highly accurate, the given data has not yet been verified using field data. Indeed, the initial condition often does not match the recorded value, leading to an immediate error simply due to unverified data at the start time of the model. Although initial salinity recorded data varies spatially around 35 ppt, the TXBLEND model yields an obviously lower value for the case of "tcSALT01" as in Figure 11, and differing values in the remaining recording stations.

We note that the effects of evaporation can lead to increasingly higher salinity values, especially in the areas surrounding Laguna Madre. However, the input of freshwater from precipitation and riverine inflow will decrease these values. The data supplied for spatially constant evaporation does

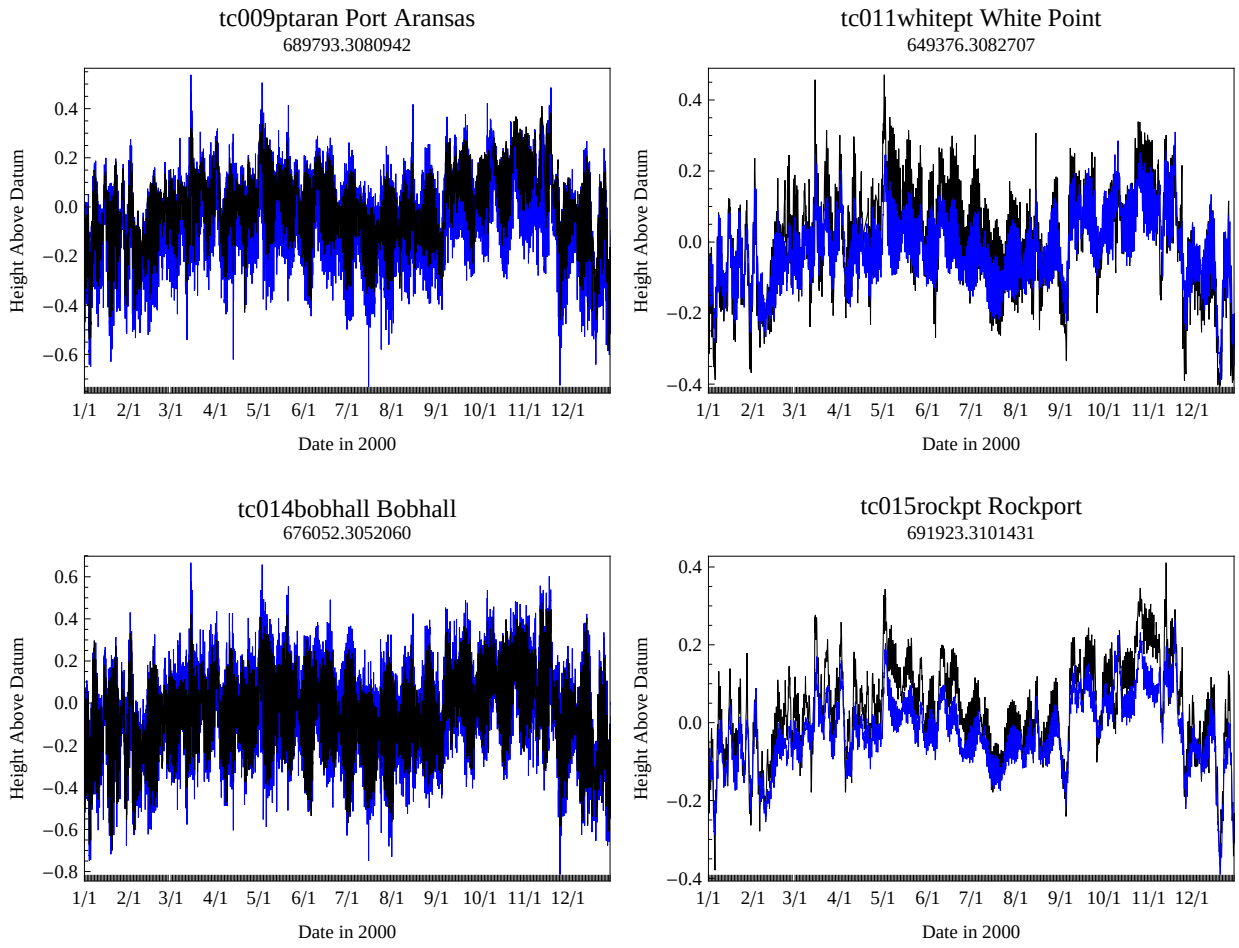

Figure 8: Water elevation comparisons at "tc" locations

not appear to sufficiently counter these mixing effects (see Figure 5). Indeed, a strongly positive fresh water balance that clearly corresponds to values of salinity much smaller than 30ppt contradict salinity measurements at the recording stations. This leads us to believe that the input data is simply not sufficiently accurate nor complete to provide a true and accurate comparison between recorded and modelled data.

Regarding a vertical convergence test, we ran two specific cases: a one-layer and a ten-layer simulation between January and May 2000. The results of these tests match in a visual context; this is demonstrated in Figure 13 at three selected individual points. In view of the shallow bathymetry and well mixed flow in this test problem, we are not surprised that our results do not change substatially with a number of layers greater than one.

4.2.3 Temperature

For this test problem, temperature is initially constant baywide at 20 and remains constant throughout the simulation.

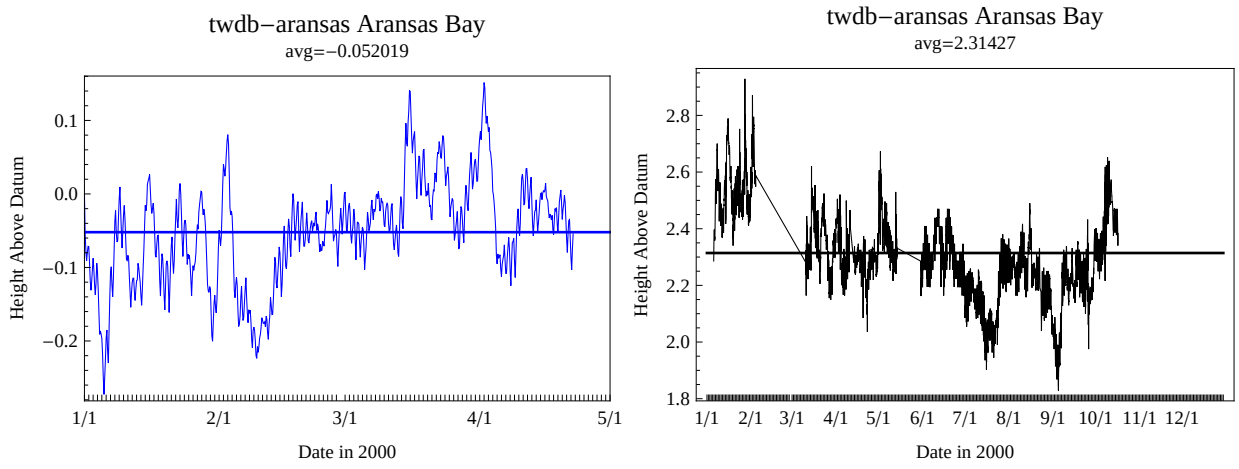

Figure 9: Zoom of water elevation average values at Aransas

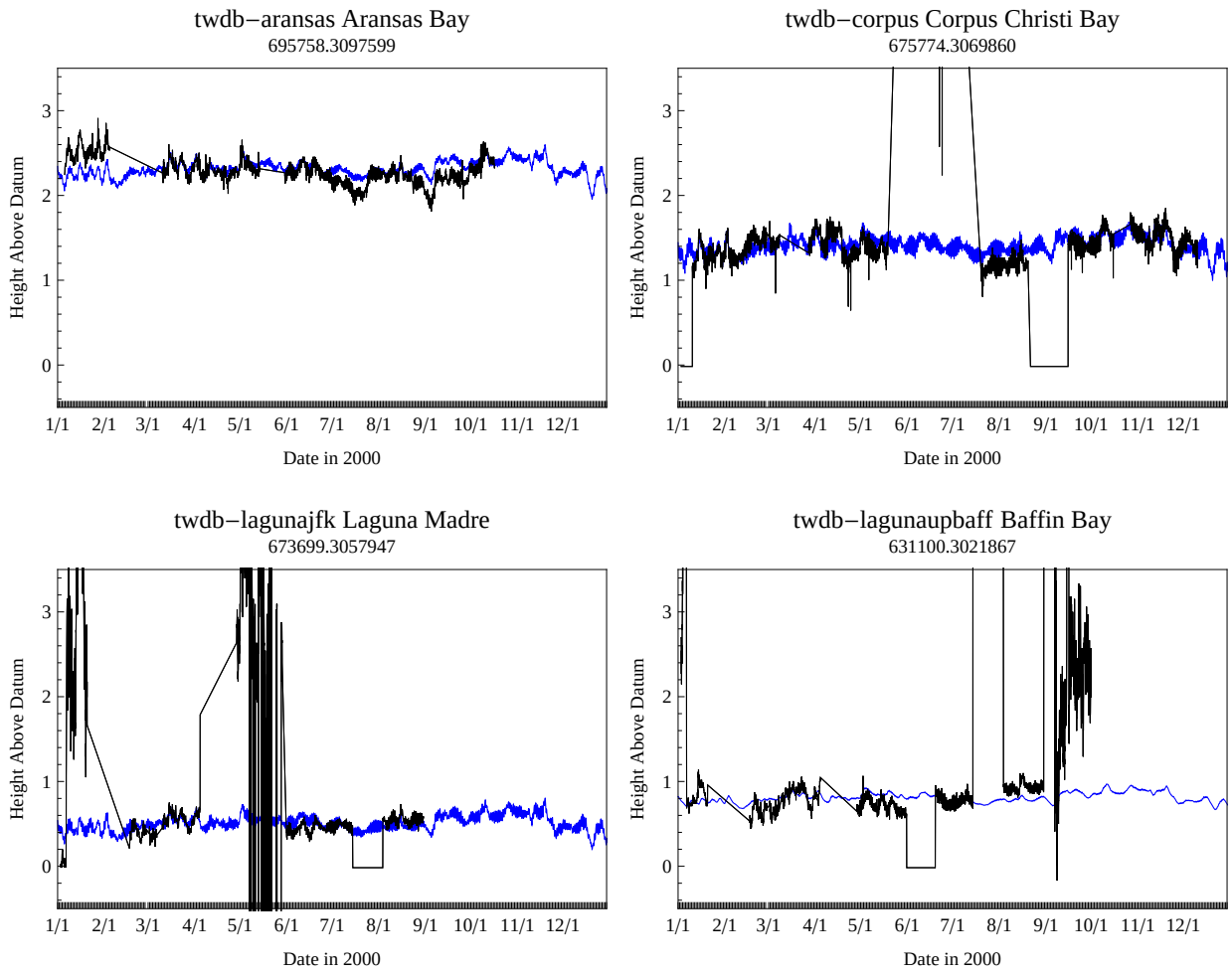

Figure 10: Water elevation comparisons at “twdb” locations: shifted

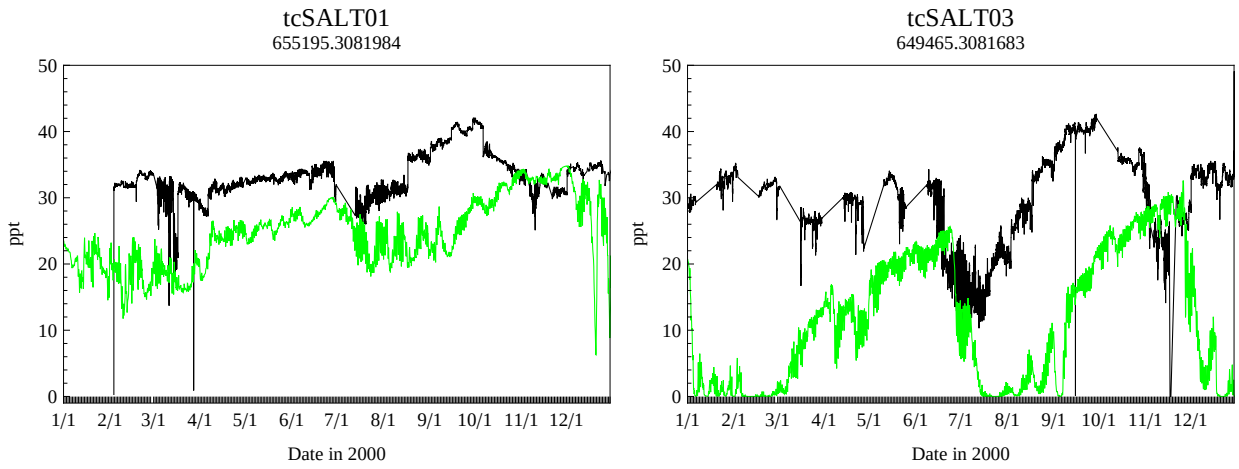

Figure 11: Salinity comparisons at "tc" locations

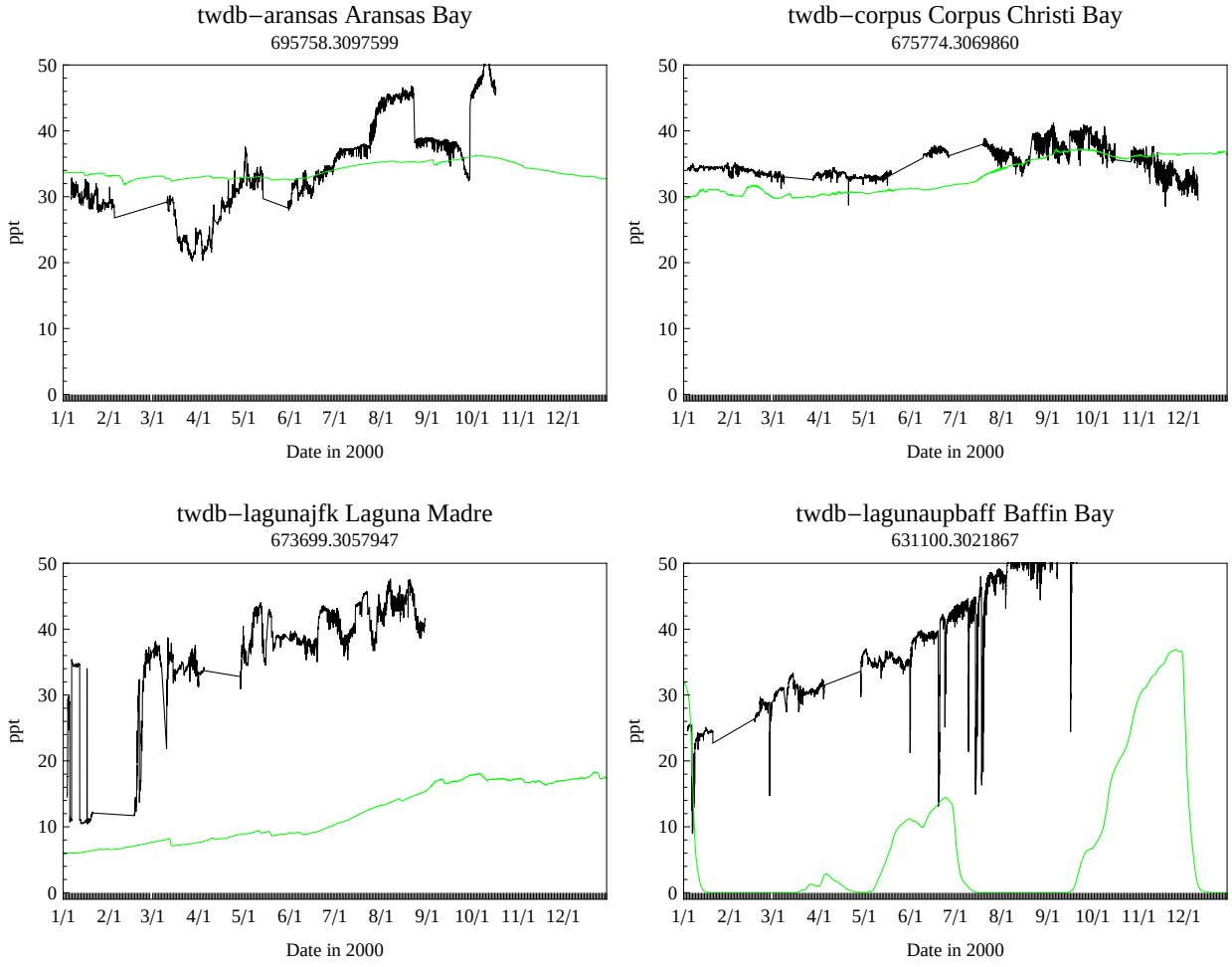

Figure 12: Salinity comparisons at "twdb" locations

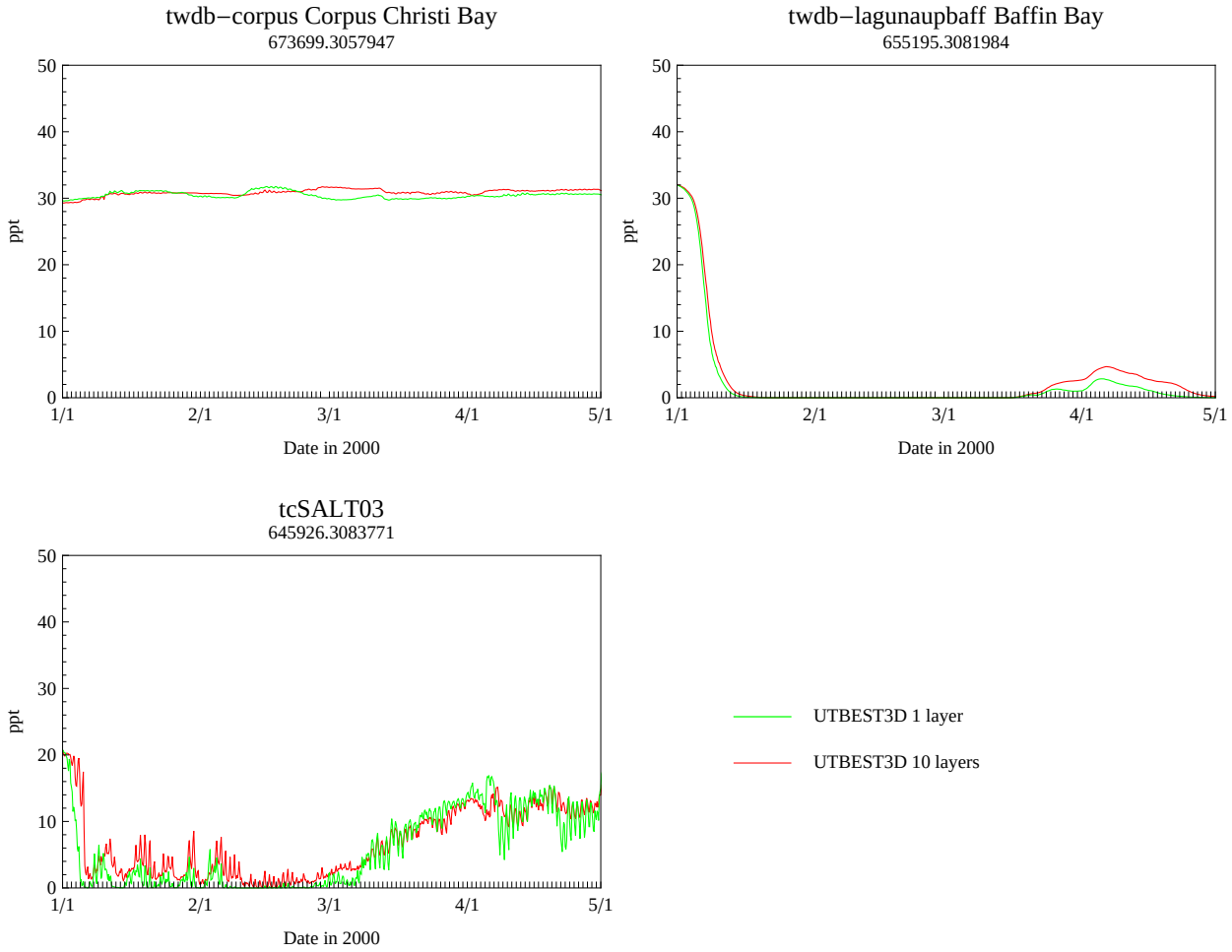

Figure 13: Salinity comparison of 1 to 10 layer simulations at select locations

4.3 Midgewater Survey Verification Study results

The Texas Water Development Board conducted Corpus Chisti Bay Intensive Inflow Survey for the time period of May 5-7, 2000, the resuls of which can be found online. Among the quantities surveyed are the water velocity magnitudy, velocity angle, and water quality in terms of salinity values. We compare our results a site 1A (Entrance Channel at UTMSI) and site 3A (CC Channel at Harbor Bridge). A map of this area is displayed in figure 14.

4.3.1 Water quality

We conduct vertical salinity profile comparisons of a 10 layer UTBEST3D simulation to this surveyed data at select times between May 5-7, 2000 at site 3A (salinity data from site 1A was not available). We select four specific times, equally spaced within the timeframe, and present the results in Figure 15. The numerical and recorded data values at zero depth in each figure are within 2-3 ppt of eachother at around 33 ppt. The salinity profile of the recorded data, as the depth progresses down to approximately 60 feet, tends to a slightly higher value, reaching 35 to 36 ppt. In contrast, the simulated data appears to remain at a constant value of approximately 33 ppt regardless of depth. We note, however, that in fact the UTBEST3D results also drift towards

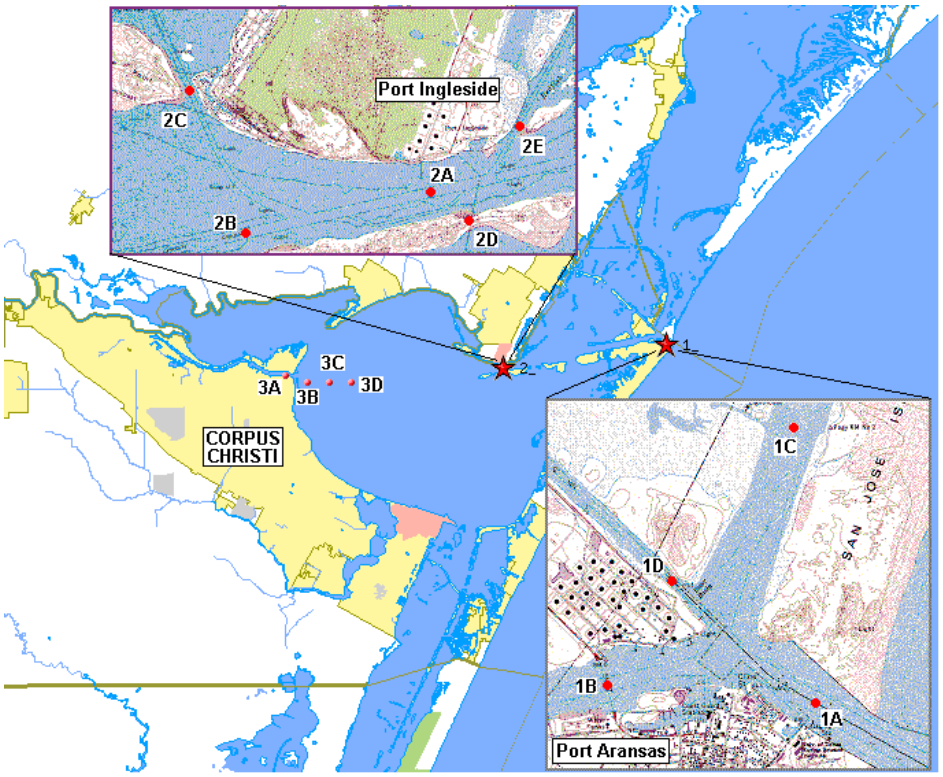

Figure 14: Map of Midgewater Survey location

(very) slightly higher salinity values as the depth progresses. This is evident in Figure 16 where the scaling of the plot has been changed to demonstrate this phenomena.

Note that the measuring station is located in a channel and therefore may have very fast mixing. The nearly constant depth variations in our model have two possible explanations. The mixing representation by our vertical eddy viscosity model could perhaps be improved by experimenting with different parametric values. Secondly, note that we perform a numerical slope limiting on the salinity variables; this could dampen the values somewhat. Nonetheless, our results are overall in fairly good agreement with recorded data at this particular location and timesnaps.

4.3.2 Velocity magnitude and direction

Velocity comparisons exhibit some interesting characteristics. Clearly the resuls at site 1A match very well between the computed and recorded survey data. The phase of both the magnitude and direction is captured very well by our model. However, the comparison at site 3A yields poor results. We contribute this to he fact that although site 1A is located in a larger water body near Port Aransas, site 3A is in a small channel that is not well defined in the mesh.

5 Conclusions

In this report, we have described recent developments and a specific application of the simulator UTBEST3D in which comparisons of real-world recorded data to numerical results are presented. The code was applied to a baroclinic simulations of the Corpus Christi Bay region, extending from Baffin Bay to Aransas and Copano Bays. Grid, elevation, wind and evaporation, and velocity data

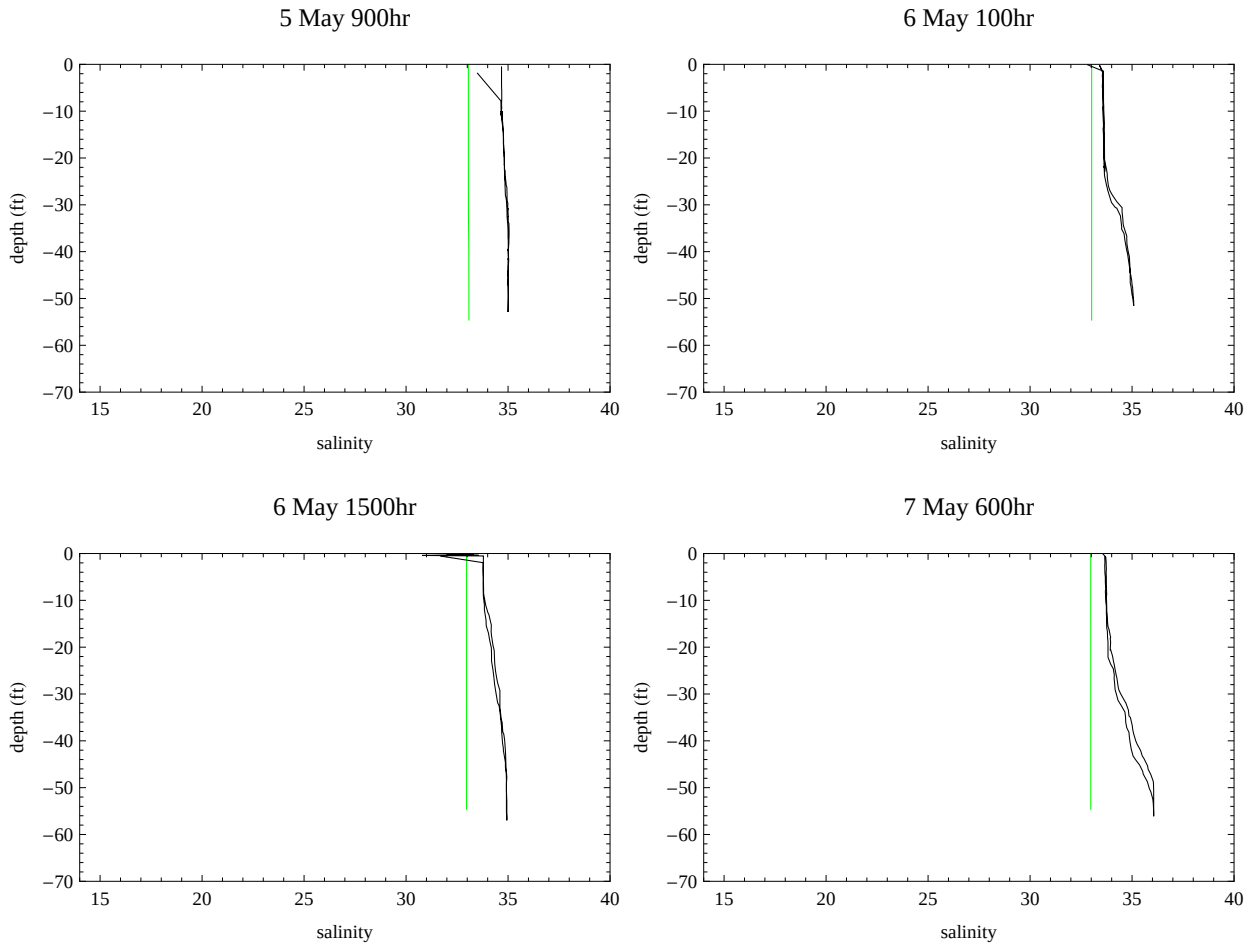

Figure 15: Salinity depth profile comparison of UTBEST3D 10 layer run to Midgewater survey data at select times

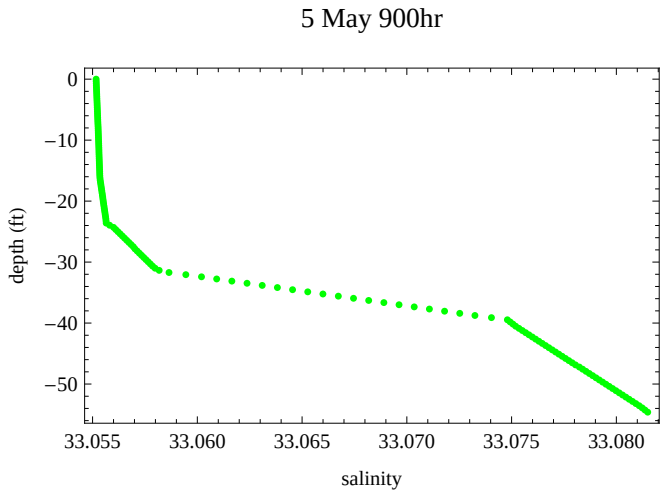

Figure 16: Zoom UTBEST3D salinity depth profile of 10 layer run at Midgewater station 3A.

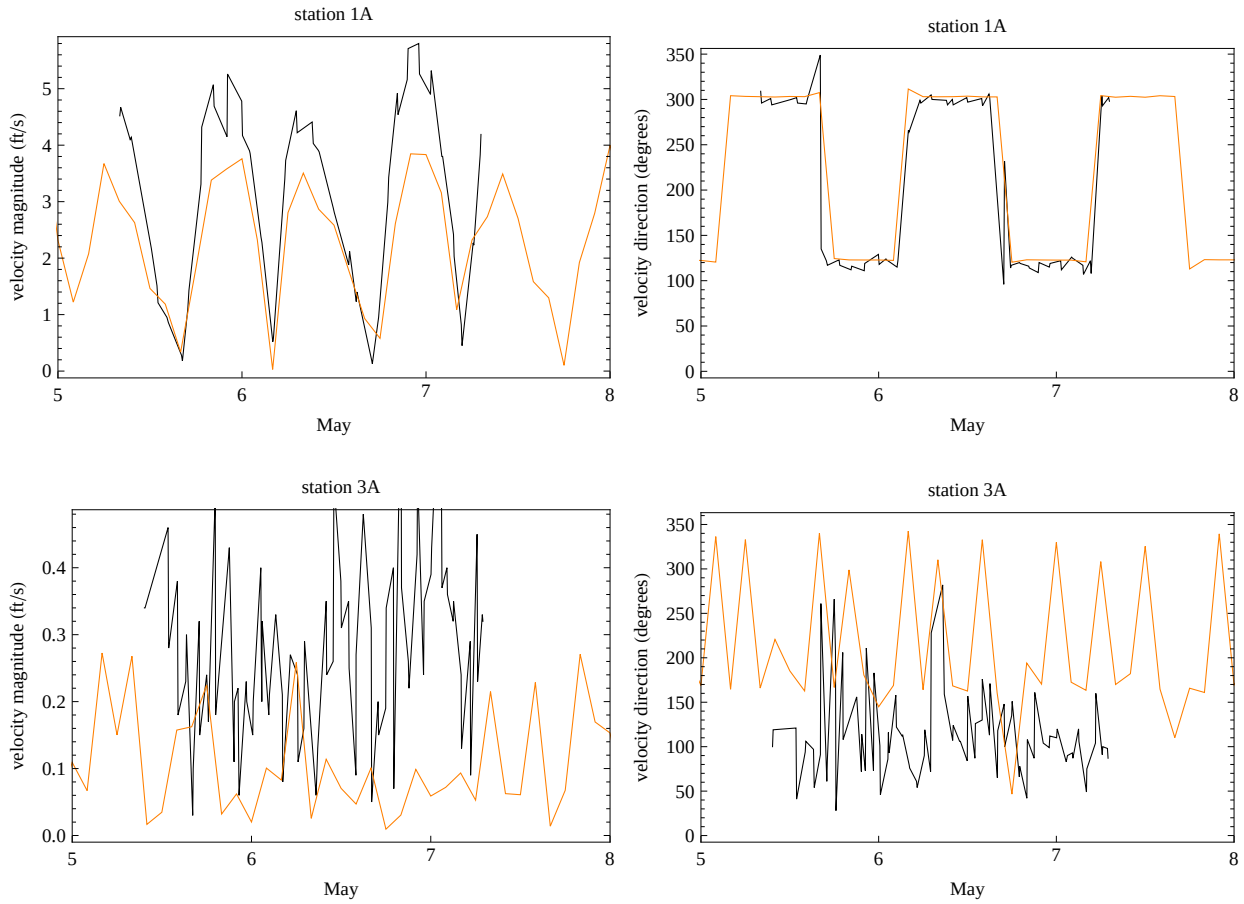

Figure 17: Velocity magnitude and angle comparisons to surveyed data

are obtained for the year 2000 for these studies from TWDB. We conclude that water elevation and velocity comparisons between recorded data and modeled results display good quanititative agreement, but that salinity values are inconsistent, leading us to believe that input data is not sufficiently accurate. However, upon verification of the model based on these comparisons and assumptions, a simulation of the region for the year 2001 was conducted, and resulting data supplied to TWDB personnel. Additionally, a description of the input parameters was supplied for the purposes of inter-model comparisons.

6 Bibliography

References

[1] V. Aizinger, C. Dawson, *A discontinuous Galerkin method for two-dimensional flow and transport in shallow water*, Advances in Water Resources, 25, pp. 67-84, 2002.

[2] V. Aizinger, C. Dawson, *The local discontinuous Galerkin method for three-dimensional shallow water flow*, Comp. Meth. Appl. Mech. Eng., 196, pp. 734–746, 2007.

[3] Burchard, H., Bolding, K., *Comparative analysis of four second-moment turbulence closure models*, Ocean Model., 3, pp 33-50, 2001.

[4] S. Chippada, C. N. Dawson, M. Martinez, M. F. Wheeler, *A Godunov-type finite volume method for the system of shallow water equations*, Comput. Meth. Appl. Mech. Engrg., 151, pp. 105-129, 1998.

[5] B. Cockburn, G. Karniadakis and C.-W. Shu, *The development of discontinuous Galerkin methods*, in Discontinuous Galerkin Methods: Theory, Computation and Applications, B. Cockburn, G. Karniadakis and C.-W. Shu, editors, Lecture Notes in Computational Science and Engineering, volume 11, Part I: Overview, pp.3-50, Springer, 2000.

[6] B. Cockburn, C.-W. Shu, *The local discontinuous Galerkin finite element method for convection-diffusion systems*, SIAM J. Numer. Anal., 35, pp. 2440-2463, 1998.

[7] A. M. Davies, *A three-dimensional model of the Northwest European continental shelf, with application to the M4 tide*, J. Phys. Oceanogr., 16(5), pp. 797-813, 1986.

[8] C.Dawson, V.Aizinger, *A Discontinuous Galerkin Method for Three-Dimensional Shallow Water Equations*, Journal of Scientific Computing, to appear.

[9] *Delft3D-FLOW User Manual*, WL—Delft Hydraulics, 2005.

[10] G. Karypis and V. Kumar, *A fast and high quality multilevel scheme for partitioning irregular graphs*, SIAM J. Sci. Comp., 20, pp. 359–392, 1999.

[11] http://mason.gmu.edu/ bklinger/seawater.pdf.

[12] Mellor, G.L., Yamada, T., *Development of a turbulence closure model for geophysical fluid problems*, Rev. Geophys. Space Phys., 20, pp. 851-875, 1982.

[13] Umlauf, L., Burchard, H., *A generic length-scale equation for geophysical turbulence models*, J. Marine Res., 61, pp 235-265, 2003.

[14] C. B. Vreugdenhil, *Numerical Methods for Shallow-Water Flow*, Kluwer, 1994.

[15] Warner, J.C., Sherwood, C.R. Arango, H.G., Signell, R.P., *Performance of four turbulenc closure models implemented using a generic length scale method*, Ocean Modeling, 8, pp. 81-113, 2005.

[16] Saffman, P.G., Wilcox, D.C., *Turbulence-model predictions for turbulent boundary layers*, AIAA J. 12(4), pp. 541-546, 1974.

[17] Zhang, Y.-L., Baptista, A.M. and Myers, E.P. *A cross-scale model for 3D baroclinic circulation in estuary-plume-shelf systems: I. Formulation and skill assessment*, Cont. Shelf Res. 24, pp. 2187-2214, 2004.